Superheating and supercooling of Ge nanocrystals embedded in SiO_2

Q. Xu,[1,2] I.D. Sharp,[1,2] C.W. Yuan,[1,2] D.O. Yi,[1,2] C.Y. Liao,[1,2] A.M. Glaeser,[1,2] A.M. Minor,[4] J.W. Beeman,[1] M.C. Ridgway,[5] P. Kluth,[5] J.W. Ager III,[1] D.C. Chrzan,[1,2] and E.E. Haller[1,2,*]

[1] Materials Sciences Division, Lawrence Berkeley National Laboratory, Berkeley, CA 94720, USA
[2] Department of Materials Science and Engineering, University of California, Berkeley, CA 94720 USA
[3] Lawrence Livermore National Laboratory, Livermore, CA 94550, USA
[4] National Center for Electron Microscopy , Lawrence Berkeley National Laboratory, Berkeley, CA 94720, USA
[5] Department of Electronic Materials Engineering, Research School of Physical Sciences and Engineering, Australian National University, Canberra ACT 0200, Australia

[*] Email: eehaller@lbl.gov

Abstract. Free-standing nanocrystals exhibit a size-dependant thermodynamic melting point reduction relative to the bulk melting point that is governed by the surface free energy. The presence of an encapsulating matrix, however, alters the interface free energy of nanocrystals and their thermodynamic melting point can either increase or decrease relative to bulk. Furthermore, kinetic contributions can significantly alter the melting behaviours of embedded nanoscale materials. To study the effect of an encapsulating matrix on the melting behaviour of nanocrystals, we performed *in situ* electron diffraction measurements on Ge nanocrystals embedded in a silicon dioxide matrix. Ge nanocrystals were formed by multi-energy ion implantation into a 500 nm thick silica thin film on a silicon substrate followed by thermal annealing at 900 °C for 1 h. We present results demonstrating that Ge nanocrystals embedded in SiO_2 exhibit a 470 K melting/solidification hysteresis that is approximately symmetric about the bulk melting point. This unique behaviour, which is thought to be impossible for bulk materials, is well described using a classical thermodynamic model that predicts both kinetic supercooling and kinetic superheating. The presence of the silica matrix suppresses surface pre-melting of nanocrystals. Therefore, heterogeneous nucleation of both the liquid phase and the solid phase are required during the heating and cooling cycle. The magnitude of melting hysteresis is governed primarily by the value of the liquid Ge/solid Ge interface free energy, whereas the relative values of the solid Ge/matrix and liquid Ge/matrix interface free energies govern the position of the hysteresis loop in absolute temperature.

1. Introduction

It has long been known that as the size of a nanocrystal decreases, the melting point is altered due to the large contribution of the surface free energy to the total energy of the system [1,2]. For the case of free-standing nanocrystals, the thermodynamic melting point varies linearly with the inverse of the particle radius as [3-5]:

$$T_m(r) - T_m^{bulk} \propto \frac{T_m^{bulk}}{Lr}\left[\left(\frac{\rho_{nc(S)}}{\rho_{nc(L)}}\right)^{2/3}\gamma_{nc(L)/vac} - \gamma_{nc(S)/vac}\right] \quad (1)$$

where $T_m(r)$ is the size-dependent melting point of the nanocrystal, T_m^{bulk} is the bulk melting point, L is the latent heat of fusion, r is the particle radius, ρ is the density of each phase and γ_i is the interfacial energy of interface i. Experimental observations of the melting points of both metal [3] and semiconductor nanocrystals [6] are in excellent agreement with the predictions of Eq. 1. For all known materials, the bracketed term in Eq. 1 is less than zero and the melting points of nanocrystals are depressed relative to the bulk value, often by hundreds of degrees.

For the case of nanocrystals embedded in a host matrix, the thermodynamic melting points also vary with the particle radius. However, Eq. 1 must be modified; surface free energies must be replaced by interfacial energies and the geometrical confinement of the particles must be accounted for. In this case, the melting point varies with particle radius according to:

$$T_m(r) - T_m^{bulk} \propto \frac{T_m^{bulk}}{Lr}\left[\gamma_{nc(L)/matrix} - \gamma_{nc(S)/matrix}\right]. \quad (2)$$

In contrast to the case of free-standing nanocrystals, the thermodynamic melting points of matrix-embedded nanocrystals may be either enhanced or depressed relative to the bulk melting point because the bracketed term in Eq. 1 may be either positive or negative. In this work, we originally sought to determine the thermodynamic melting points of Ge nanocrystals embedded in silica. We will show, however, that it is necessary to invoke kinetics to describe the melting behaviors of these nanocrystals. Due to the values of the interfacial energies $\gamma_{Ge(L)/Ge(S)}$, $\gamma_{Ge(L)/silica}$, and $\gamma_{Ge(S)/silica}$ it is necessary to nucleate both the liquid and solid phases during melting and solidification, respectively. Thus, these phase transformations are activated processes that lead to both kinetic superheating and supercooling in the same system.

2. Experimental

Ge nanocrystals were formed by ion implantation of ^{74}Ge into 500 nm thick silica thin films on Si substrates. Multi-energy implantation was performed at 120 keV to 2×10^{16} cm^{-2}, 80 keV to 1.2×10^{16} cm^{-2}, and 50 keV to 1×10^{16} cm^{-2}. Nanocrystal growth was achieved by thermal annealing at 1173 K for 1 h under Ar, followed by rapid cooling from the growth temperature.

Melting points of nanocrystals were determined by *in situ* heating in a JEOL 3010 microscope equipped with a Gatan 628Ta single tilt heating holder. Samples were heated and cooled between room temperature and 1473 ± 15 K in 15 K increments and electron diffraction patterns were collected at each temperature after 5 min of temperature stabilization. Radial integration of the powder-like diffraction patterns from the randomly-oriented Ge nanocrystals was used to monitor the crystallinity at each temperature. Multiple temperature cycles were performed on individual samples and experiments were repeated on multiple samples; all results were identical within the experimental error.

To ensure the validity of temperature measurement, and exclude effects of temperature lag during heating and cooling, the melting point of Au nanocrystals with an average diameter of 5 nm was measured under identical conditions. Au nanocrystals were formed in a 500 nm thick silica thin film on a silicon substrate by ion beam synthesis. Melting occurred at the expected temperature, thus confirming the accuracy of temperature measurement during Ge nanocrystal measurements.

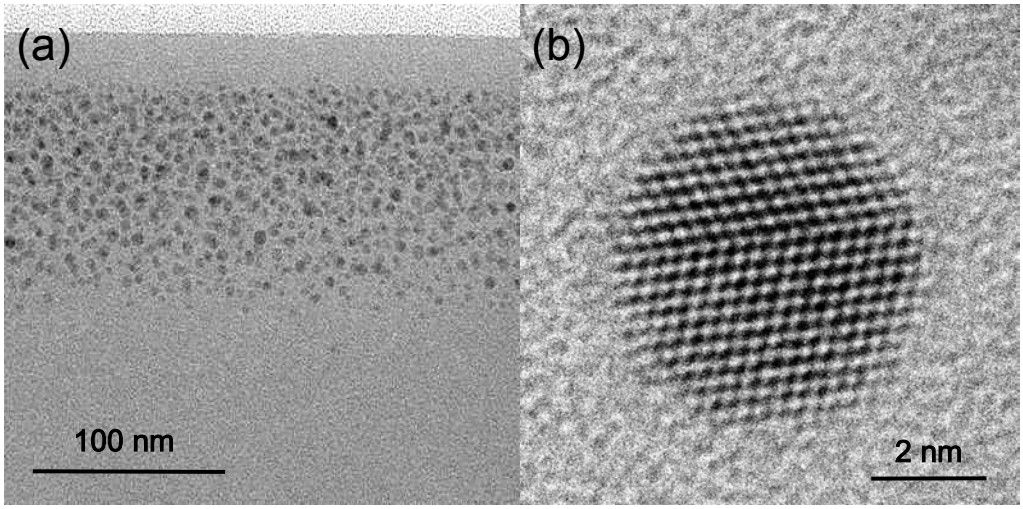

Figure 1: Transmission electron micrographs showing silica-embedded Ge nanocrystals. (a) Low magnification image showing a band of Ge nanocrystals in the implanted zone near the surface of the sample. (b) High resolution image of an individual 5.3 nm diameter Ge nanocrystal with a single twinning plane. All nanocrystals in the present work are spherical with sharp interfaces to the surrounding matrix.

3. Results

Figure 1 shows transmission electron microscope (TEM) images of silica-embedded Ge nanocrystals after thermal annealing. Image analysis of low magnification TEM images, such as that shown in Fig. 1(a), reveals that the nanocrystals have a mean size of 5.1 nm and a distribution full width at half maximum (FWHM) of 3.4 nm. A high resolution TEM (HR-TEM) image of an individual nanocrystal is shown in Fig. 1(b). Embedded nanocrystals are spherical and have sharp interfaces with the surrounding silica matrix.

The integrated intensities of the Ge diffraction peaks as a function of temperature during a single heating and cooling cycle are given by the data points in Fig. 2. During heating, melting is not observed until well above the bulk Ge melting temperature of 1211 K. Indeed, significant diffraction intensity is observed up to ~1400 K, almost 200 K above the bulk Ge melting point. During cooling from the molten state, however, Ge diffraction rings do not reappear until ~930 K, well below the bulk Ge melting point. Thus, silica-embedded Ge nanocrystals exhibit a ~470 K melting and solidification hysteresis located around the bulk melting point during a single thermal cycle. This result is reproducible during multiple heating and cooling cycles of a single sample and on measurements of multiple different samples.

4. Discussion

Although equilibrium theory predicts that the melting points of embedded nanocrystals may be either enhanced or suppressed relative to bulk, it cannot account for a melting point hysteresis. Therefore, we consider the possibility of kinetically-limited melting and solidification. Supercooling is commonly observed and is a consequence of the activation barrier associated with formation of a solid/liquid interface upon nucleation of a solid cluster while cooling a molten material [7].

In principle, kinetically-limited melting is also possible during heating of a solid. However, superheating is not experimentally observed for the case of bulk materials or free-standing nanocrystals due to surface pre-melting. For all known materials, the interfacial free energy balance $\gamma_{S/L} + \gamma_{L/vac} < \gamma_{S/vac}$ holds and it is energetically favorable for a very thin liquid film to form over the solid surface as the melting point is approached. Consequently, there is no nucleation barrier for formation of the liquid phase and the transformation from solid to liquid occurs at the thermodynamic

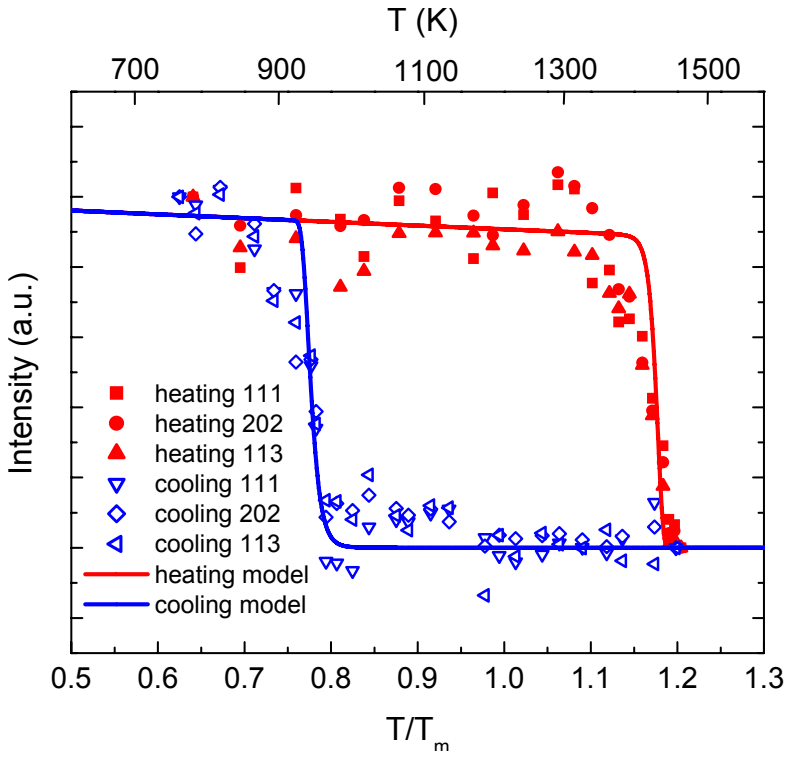

Figure 2: Data points show the normalized integrated diffraction intensity as a function of temperature during a single heating and cooling cycle. A melting and solidification point hysteresis of ~470 K is observed. The solid lines show the diffraction intensity as a function of temperature during heating and cooling calculated according to the kinetic theory described in the text.

melting point. We note that small superheating effects can occur, relative to the depressed equilibrium melting point, for the case of free-standing nanocrystals. Couchman and Jesser [4] first considered this possibility and found small enhancements relative to predicted size-dependent thermodynamic melting point due to a maximum of the total free energy as a function of the liquid fraction of the particle. However, in no case was the melting point enhanced above the bulk equilibrium melting point.

For an embedded nanocrystal, a wider range of possible behaviors exists because the relative value of the interfacial energies depends upon the materials system. If $\gamma_{nc(S)/nc(L)} + \gamma_{nc(L)/matrix} > \gamma_{nc(S)/matrix}$, then surface pre-melting will not occur, nucleation of the liquid phase will be necessary, and superheating should be observed. If, in the same materials system, $\gamma_{nc(S)/nc(L)} + \gamma_{nc(S)/matrix} > \gamma_{nc(L)/matrix}$ then nucleation of the solid phase is required for solidification and supercooling should be observed. Based upon these considerations, we have developed a quantitative theoretical model to describe the experimentally observed melting and solidification hysteresis for Ge nanocrystals embedded in silica.

Standard theory for heterogeneous nucleation, modified to account for size-dependent equilibrium melting points of nanocrystals and the spherical geometry, is applied to *both* the melting and solidification of Ge nanocrystals to define the energy barriers associated with forming critical nuclei for transformations. The transformation temperature is determined by specifying that a nucleation rate for overcoming the activation barrier to formation a critical nucleus of 1 s^{-1} is experimentally observable. However, we note that the nucleation rate has a threshold behavior with temperature and is, therefore, not strongly dependent on the rate at which the temperature is ramped during the experiment.

According to this theory, the width of the melting and solidification loop is determined primarily by the value of $\gamma_{Ge(L)/Ge(S)}$ and its position is determined primarily by the values of $\gamma_{Ge(L)/matrix}$ and $\gamma_{Ge(S)/matrix}$. We find that values of $\gamma_{Ge(L)/Ge(S)} = 0.26$ J/m^2 and $\gamma_{Ge(S)/matrix} = \gamma_{Ge(L)/matrix} = 0.91$ J/m^2, corresponding to activation energy barriers of 3.91 eV and 2.65 eV for melting and solidification, respectively, describe the experimental data well. Figure 2 shows the normalized integrated diffraction patterns obtained during *in situ* heating and cooling (data points) compared to the theory for superheating and supercooling of Ge nanocrystals (solid lines). The calculated diffraction intensity includes the effect of the Debye-Waller factor and incorporates the known nanocrystals size distribution with a r^6 dependence of the particle size on the diffraction intensity. The agreement between experiment and theory is excellent and we conclude that melting and solidification of silica-embedded Ge nanocrystals are kinetically-limited and give rise to both superheating and supercooling.

5. Conclusion

In situ electron diffraction measurements on silica-embedded Ge nanocrystals reveal a melting and solidification hysteresis of ~470 K located around the bulk Ge melting point. This behaviour, which is not expected for bulk materials and cannot be described by thermodynamic melting of nanocrystals, is assigned to kinetically-limited superheating and supercooling during melting and solidification, respectively. A quantitative theory for this behaviour, using standard heterogeneous nucleation theory, describes the experimental observations well. This model should be generally applicable to the melting of embedded nanoscale materials if the relevant interfacial energies are known.

Acknowledgements

This work was supported in part by the Director, Office of Science, Office of Basic Energy Sciences, Division of Materials Science and Engineering, of the U.S. Department of Energy under contract No. DE-AC02-05CH11231 and in part by U.S. NSF Grant No. DMR-0405472.

References

[1] P. Pawlow, Z. Phys. Chem. **65**, 1 (1909).
[2] M. Takagi, J. Phys. Soc. Jap. **9**, 959 (1954).
[3] P. Buffat and J.-P. Borel, Phys. Rev. A **13**, 2287 (1976).
[4] P. R. Couchman and W. A. Jesser, Nature **269**, 481 (1977).
[5] F. Baletto and R. Ferrando, Rev. Mod. Phys. **77**, 371 (2005).
[6] A. N. Goldstein, C. M. Echer and A. P. Alivisatos, Science **256**, 1425 (1992).
[7] D. Turnbull and R. E. Cech, J. Appl. Phys. **21**, 804 (1950).